

# Joining Ceramics before Firing by Ultrasonic Welding

H. Rashid, K. N. Hunt & J. R. G. Evans

Department of Materials Technology, Brunel University, Uxbridge, Middlesex UB8 3PH, UK

(Received 11 February 1991; revised version received 14 May 1991; accepted 24 May 1991)

## Abstract

*An ultrasonic welding method has been applied to the joining of ceramic suspensions suitable for injection moulding, extrusion or other plastic forming operations in order that greater complexity of form can be achieved. Scanning electron microscopy shows that interfaces free from welding defects after binder removal and sintering can be obtained. However, considerable difficulties were experienced in welding the highly filled suspensions and these are discussed in terms of ultrasonic attenuation, enhanced thermal diffusivity and changes in coefficient of friction. The feasibility of the method has been established but it has not been optimized.*

*Zur Erzielung höherer Bauteilkomplexität wurden keramische Formteile, die durch Spritzguß, Extrudieren oder andere plastische Formgebungsverfahren aus Suspensionen hergestellt wurden, mittels einer Ultraschallfügetechnik verschweißt. Rasterelektronenmikroskopische Aufnahmen zeigen an den Fügstellen nach der Entfernung des Binders und nach dem Sintern keinerlei Anzeichen von Gefügefehlern. Jedoch ergaben sich beträchtliche Schwierigkeiten beim Fügen von Suspensionen mit hohem Feststoffanteil. Diese Probleme werden im Hinblick auf das Dämpfungsverhalten, erhöhte Temperaturleitfähigkeit und Änderungen des Reibungskoeffizienten diskutiert. Die Einsatzmöglichkeit des Verfahrens konnte nachgewiesen werden. Es bedarf jedoch noch der Optimierung.*

*On montre l'intérêt d'une méthode de soudure ultrasonique pour la jonction de pièces céramiques 'cruës', obtenues à partir de suspensions. Cette méthode est applicable pour le moulage par injection, l'extrusion et d'autres opérations de mise en forme*

*plastique, dans le but d'atteindre des géométries plus complexes. L'étude MEB montre que l'on peut obtenir, après déliantage et frittage, des interfaces ne présentant pas de défauts de soudure. On rencontre toutefois, dans le cas de suspensions très chargées, des difficultés considérables, lesquelles sont abordées sous l'angle de l'atténuation ultrasonique, d'une diffusibilité thermique améliorée et des modifications du coefficient de friction. On a démontré la faisabilité de la méthode, il reste à l'optimiser.*

## 1 Introduction

Ceramic fabrication operations which involve the plastic forming of a suspension include injection moulding,<sup>1</sup> post-extrusion forming,<sup>2</sup> vacuum forming<sup>3</sup> and blow moulding.<sup>4</sup> Even greater complexity of form is possible if such shapes can be joined before firing and both solvent welding<sup>5</sup> and butt fusion welding<sup>6</sup> have been demonstrated.

Ultrasonic welding of polymers has an advantage over other joining methods of speed and automation. The weldment is formed often in a fraction of a second as a result of heat generated at the interface by local ultrasonic absorption and friction. In thermoplastics, the strength of the joint is generally interpreted in terms of the interdiffusion of polymer segments across the interface.<sup>7</sup> As with the other operations for joining of suspensions, provided the particles are uniformly dispersed, the intimate molecular contact associated with the welding of the organic phase should be accompanied by particle arrangement across the interface which allows sintering.

Ultrasonic welding machines operate in the 20–35 kHz region with input power up to 3 kW using ceramic piezoelectric transducers which provide

conversion efficiencies up to 95%.<sup>8</sup> Weld times are in the range 0.1–3 s making the procedure attractive for mass production operations on polymer products. The work pieces are lightly clamped and the sonotrode brought into contact with a force in the range 20–1800 N, pneumatically controlled.<sup>8</sup> Ultrasonic energy is absorbed, *inter alia*, in the interfacial region by frictional effects resulting in local heating and melting of the thermoplastic.

Weld quality is a combination of material properties and joint design. The weldability of a range of plastics has been studied empirically and desirable material properties have been loosely identified.<sup>8</sup> It is suggested that high elastic modulus is desirable on the grounds that high modulus materials generally present low acoustic loss. Clearly this general rule does not necessarily apply to composite materials where losses may be enhanced by scattering and absorption.<sup>9</sup> Low melting temperatures are desirable to reduce the energy needed at the interface. Similarly, low specific heat and density are preferable. It is argued that a high coefficient of friction increases acoustic absorption at the interface.

Furthermore, high thermal conductivity is thought to be desirable<sup>8</sup> but the reason is not clear. On the contrary, a high thermal conductivity would give rise to rapid heat transfer away from the interfacial region thus extending the weld time and heating the adherends. Ceramic-filled polymers would be expected to present this problem.

The main welding parameters are amplitude, weld pressure, weld time and hold time. Amplitude affects the amount of energy dissipated and should be as high as possible without causing damage to the components. Weld strength generally increases with weld time and with increased pressure, however, excessive pressure can cause a reduction in strength attributable to molecular orientation in the flow direction.<sup>10</sup> As well as the rapid automated production that is possible for ultrasonic welding of thermoplastics, joint strengths typically approach 95% of the strength of the parent material.<sup>11</sup>

Joint design is also identified as an influential feature in ultrasonic welding. A small prismatic ridge on one adherend, a so called 'energy director' is regarded as concentrating ultrasonic absorption and initiating flow.<sup>12</sup> Joints can be designed for 'direct' or near-field welding and 'indirect' or far-field welding. In the former, preferred for amorphous polymers, the sonotrode is within about 6 mm of the interface while in the latter the ultrasound is transmitted over large distances to the weld surfaces.

In the present work, near-field welding experi-

ments were carried out on samples without an energy director and with a machine supplying a fixed amplitude suitable for welding polymers. No attempts were made to optimize machine or joint design parameters for the particular materials to be welded. Such tasks rest rightfully with those skilled in the art; there being a high empirical content to the knowledge base of ultrasonic welding experts. Since polystyrene is easily welded under a wide range of conditions, all the suspensions investigated used polystyrene as a main binder component. The type of ceramic and its volume fraction were varied and an attempt was made to understand the quality of welded sintered products in terms of the material property changes brought about by high filler loadings. The emphasis was placed on microscopical characterization of weld regions. The process is insufficiently developed to examine the mechanical strength of joints.

## 2 Experimental Details

### 2.1 Materials and mixing procedure

The sources of materials and compositions of suspensions are shown in Table 1. Premixing was carried out in a Henschel high speed mixer at 3000 rpm for 2 min and compounding was achieved using a Betol TS40 twin screw extruder operating at 60 rpm with barrel temperatures 200–210–220–210°C feed to exit for composition 1 and 140–160–180–190–210°C feed to die for composition 2.

### 2.2 Welding experiments

Samples for welding were cut from 2 mm sheet compression moulded at 160°C in an electrically heated hydraulic press between polyester sheet (Melinex ex ICI plc). The samples were 19 mm × 75 mm and were abraded on 400 grade silicon carbide paper to remove potential surface contamination from the polyester. A 1500 W Branson 20 kHz welding machine (Branson Sonic Power Co., Danbury, CT, USA) was used (series 800 type 5–15R). The sonotrode was 6A14Va titanium with a rectangular cross-section of area  $2.5 \times 10^{-4} \text{ m}^2$ . A range of weld times and pressures were explored. In some experiments the samples were preheated on the anvil using a warm air blower until the temperature between the adherends reached 43°C as measured by a 32 swg type K thermocouple sandwiched between the adherends. Welded sections were examined in the scanning electron microscope (Cambridge S250) after pyrolysis of the organic vehicle in nitrogen at 2°C/h to 450°C and sintering at 1550°C for 1 h in air.

**Table 1.** Composition of suspensions

| Constituent         | Grade              | Source                      | wt %  |
|---------------------|--------------------|-----------------------------|-------|
| Ceramic = 45 vol. % |                    |                             |       |
| 1. Zirconia         | HSY-3 <sup>a</sup> | Daichi-Kigenso Japan        | 82.40 |
| Polystyrene         | HF555              | BP Chemicals UK             | 14.66 |
| Dibutylphthalate    | GPR                | BDH Chemicals UK            | 2.93  |
| Ceramic = 54 vol. % |                    |                             |       |
| 2. Alumina          | RA6 <sup>b</sup>   | Alcan Chemicals UK          | 81.96 |
| Polystyrene         | HF555              | BP Chemicals UK             | 12.63 |
| Trimellitate ester  | OTM                | ICI Chemicals & Polymers UK | 3.61  |
| Stearic acid        | GPR                | BDH Chemicals UK            | 1.80  |

<sup>a</sup> Ultimate particle size 0.1–0.2  $\mu\text{m}$ .

<sup>b</sup> Ultimate particle size 0.3–1.6  $\mu\text{m}$ .

### 2.3 Measurement of thermal diffusivity

The unsteady state method of Beatty *et al.*<sup>13</sup> was used to measure the thermal diffusivity of polystyrene and composition 2. Two discs measuring 80 mm in diameter by 9 mm in thickness were compression moulded. The faces were then cleaned by abrasion and a 32 swg type K thermocouple was placed between them. The whole assembly was then remoulded in a jugged tool to produce an 80 × 18 mm disc with a central thermocouple. The initial temperature of the disc was recorded. Heating was achieved by a stirred water bath maintained at 80 or 85°C and the centre temperature was recorded as a function of time.

### 2.4 Assessment of attenuation

An attempt was made to measure the ultrasonic attenuation of compression moulded discs measuring 40 mm in diameter by 15 mm in length using a Portable Ultrasonic Non-Destructive Digital Indicating Tester manufactured by CNS Electronics of London. Considerable difficulty was experienced with the coupling and the result was very sensitive to applied pressure. These results are not quoted and a less direct assessment of attenuation was used. Compression moulded discs of compositions 1 and 2 and of polystyrene measuring 25.4 mm in diameter by 25 mm in length with a central radial hole were prepared under 12 MPa pressure. These were heated in the ultrasonic welder using a 2-s weld time and a hold pressure of 50 kPa. The temperature rise was measured using a 32 swg thermocouple either placed in the hole permanently or removed and replaced after ultrasonic absorption. The temperature was recorded 1 min after the ultrasonic treatment to allow preferential absorption in the vicinity of the thermocouple to decay. The average temperature rise of the three identical size components was recorded and the energy absorbed per unit volume was calculated.

### 2.5 Measurement of coefficient of friction

Pins of composition 1, 2 and of polystyrene were compression moulded in an Apex M1/R press at 12 MPa. The 8 mm pins were machined to 6 mm diameter and 15 mm length. Counterfaces of the same materials were prepared from compression moulded sheet. The surfaces were abraded on 600 grade silicon carbide paper and cleaned in an ultrasonic bath. A pin on plate reciprocating wear jig previously described<sup>14</sup> was used to obtain a dynamic coefficient of friction. A 30 mm stroke was used at a linear speed of 0.04 m/s with a load of 1 kg. The frictional force was measured by the displacement of a linear variable differential transformer transducer against a cantilever. The transducer was calibrated using a spring balance attached horizontally to the beam.

### 2.6 Measurement of specific heat

A Perkin Elmer DSC-2 was used to measure specific heat from 57°C to 200°C for both compositions and for the polystyrene. A sapphire standard was used to correct the results. A Perkin Elmer thermo-mechanical analyser was used to measure the dilatometric softening point.

## 3 Results and Discussion

### 3.1 Welding

Welding operations were carried out on a machine with amplitude and settings suitable for welding polymers. The polystyrene on which the ceramic suspensions were based was easily welded under a wide range of conditions without an energy director. The main problem with the ceramic suspensions was the brittleness conferred by the ceramic particle additions. Despite using the lightest sonotrode loading (32 N) samples tended to fracture as soon as the ultrasound was triggered. Ceramic suspensions typically have low mechanical strength<sup>15,16</sup> and it

**Table 2.** Result of welding experiments

| Composition | Weld load (N) | Weld time (s) | Preheat time (min) | Welding defects |
|-------------|---------------|---------------|--------------------|-----------------|
| 1           | 630           | 0.4           | 0                  | None            |
| 1           | 32            | 1.5           | 1.5                | None            |
| 2           | 630           | 0.8           | 0                  | None            |
| 2           | 32            | 1.0           | 1.5                | I, II; I, II    |
| 2           | 32            | 1.3           | 1.5                | I, II;          |
| 2           | 32            | 1.5           | 1.5                | I, II;          |
| 2           | 32            | 2.0           | 1.5                | I, II; I, II    |
| 2           | 130           | 1.5           | 1.5                | I, II; I, II    |
| 2           | 320           | 1.0           | 1.5                | II; none        |

appears that the amplitude of the welding machine was inappropriate for these materials. However, it was clear that fragments of the samples had welded after fracture. Thus, samples of compositions 1 and 2 were welded with loads from 32 to 630 N and weld times from 0.4 to 2.0 s. Fracture of the bulk samples took place in the majority of cases despite attention to alignment and these results are not reported. There was no facility to reduce amplitude. In Table 2, the results for two samples which were not preheated yet survived intact, are included. Preheating the samples to approximately 43°C allowed the welding process to proceed on undamaged slabs. Preheating represents an inconvenience which might be avoided by a machine which supplied lower amplitude.

Two main defect types were observed in sections. Unwelded regions which were attributed to entrapped gas were designated type I. Like the solvent<sup>5</sup> and hot plate welding<sup>6</sup> process defects, they were characterized by rounded edges which betray their origin in the molten state (Fig. 1). In between these unwelded regions it is clear that the interface is

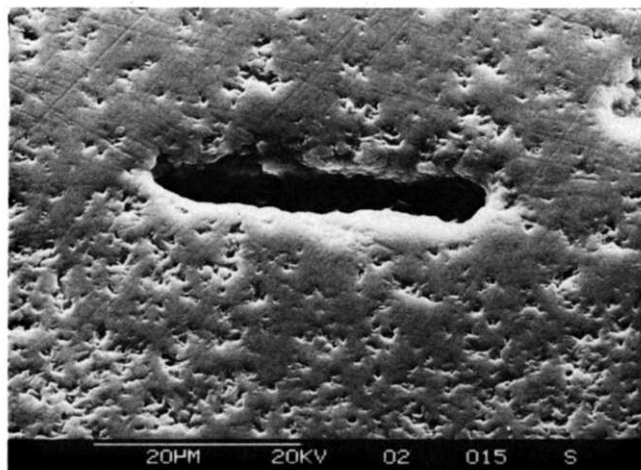


**Fig. 1.** Unwelded regions associated with entrapped gas in a sample of composition 2 welded for 1 s at 32 NPa and sintered (Type I defect). Note the sintering across the interface between the defects.

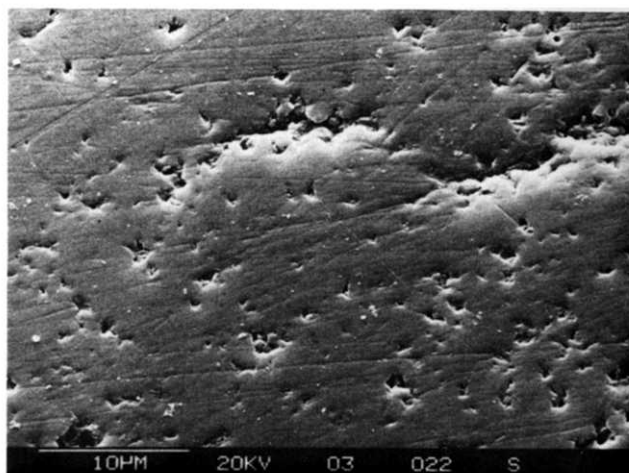


**Fig. 2.** Interfacial crack in composition 2 welded at 320 NPa for 1.0 s and sintered (Type II).

indistinguishable from the bulk after sintering and this means that the process is worthy of development. The organic vehicle has conveyed particles into sufficiently close proximity to allow particle contact at the initiation of sintering.

The second type of defect consisted of interrupted cracks at the position of the original interface which present ill-defined edges where some particle contact has taken place across the boundary and the root of the crack is partially sintered closed. These were designated type II and an example is shown in Fig. 2. Type I defects can be observed in the weld region before removal of the polymer and there is no reason to suppose that they are associated with gross phase separation under continuous wave ultrasound. The scale prevents phase separation being ruled out for type II defects but under conventional shear flow conditions, combinations of high polymers and fine powders show great reluctance to separate.

Figure 3 shows a section of a sintered alumina

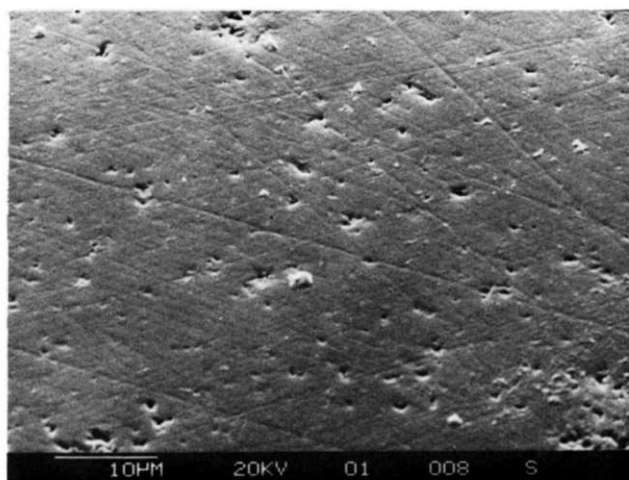


**Fig. 3.** Interfacial region in a sintered alumina sample welded at 320 NPa for 1.0 s after preheating. The actual interface cannot be located.

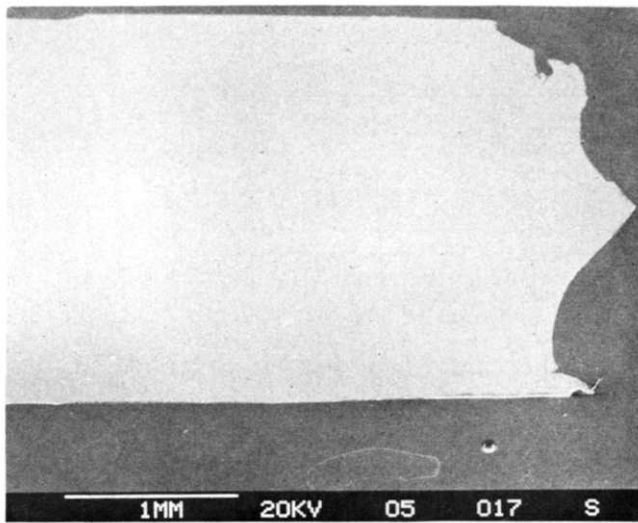


Fig. 4. Sintered  $ZrO_2$  laminate (original interface horizontal and central). No preheating was used before welding.

joint made at a weld load of 320 N and weld time of 1 s after preheating the adherends. The original interface cannot be distinguished from the bulk.

The samples of composition 1 were generally much easier to weld and this can be attributed in part to the lower ceramic volume fraction and is discussed below. Figure 4 shows a section through a sintered  $ZrO_2$  laminate. The sample cracked during welding and this crack extended through the section during binder removal but the original horizontal interface cannot be seen at this magnification. Several scans were made perpendicular to the slab in an attempt to distinguish the interfacial region. This was not possible and the microstructure was uniform across the laminate, an example being shown in Fig. 5.

The use of high loads (320–530 N), although it produced samples in which the section examined

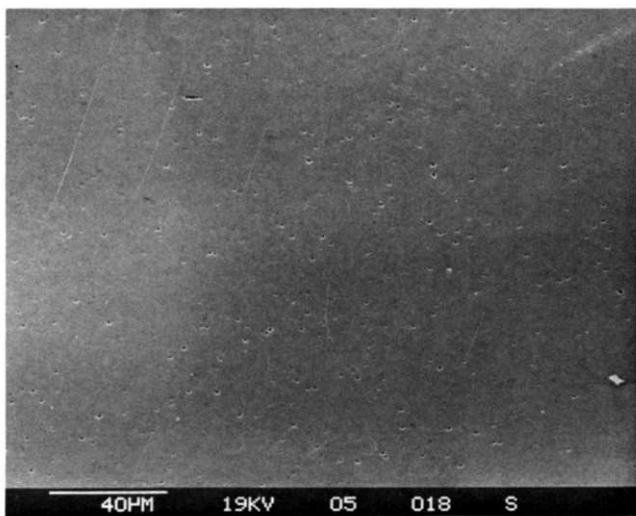


Fig. 5. The uniform sintered microstructure of the  $ZrO_2$  laminate of Fig. 4. The interface cannot be found.

was free from both types of defect, also had the unfortunate consequence that the bulk adherends were severely deformed by the sonotrode in the welded region. Thus, optimization is needed to balance the machine and material parameters.

The possible obstructions to the ultrasonic welding of filled polymers can be listed as follows. In the first place brittleness has been identified and can be overcome in several ways: by preheating the components to be welded or by improving the strength of such composites with coupling agents<sup>17</sup> or by selecting materials to enhance the acid–base interactions at the ceramic polymer interface.<sup>18</sup> In the second place, the increased thermal diffusivity of suspensions can be regarded as widening the temperature distribution around the weldline so that considerably more energy is needed to raise the local temperature at the weldline and allow flow. Thirdly, the ultrasonic attenuation in the bulk caused, *inter alia*, by scattering, may mean that the supplied energy is dissipated in the bulk rather than preferentially at the interface. Fourthly, there may be differences in the coefficient of friction caused by filler additions which mean that the interface ceases to be a good ultrasonic absorber. Fifthly, some lateral flow generally occurs in welding which would tend to promote particle motion and hence mixing at the interface. Thus one requirement for welding is a rigid solid which melts to form a low viscosity fluid. The presence of high volume loadings of ceramic causes substantial increases in viscosity<sup>19</sup> which may present an impediment to welding. Finally, it has been suggested that filled polymers are difficult to weld simply because there is not enough polymer at the interface.<sup>20</sup> This seems to be doubtful because in ceramic processing, volume loadings are chosen to allow melt flow<sup>1</sup> and extensive plastic deformation.<sup>2–4</sup> These processes require an organic content over and above that needed to fill the interstitial space<sup>21</sup> suggesting that adequate polymer is available.

### 3.2 Temperature distribution in the weld

Thermal diffusivity, measured by the method of Beatty *et al.*,<sup>13</sup> was obtained from a plot of  $\log_{10}(T_0 - t/T_0 - t_0)$  as a function of time where  $T_0$  is the water bath temperature,  $t_0$  is the initial temperature of the sample and  $t$  is the temperature after a certain time. The slope  $m$  of this line gives the average thermal diffusivity ( $\alpha$ ) over the temperature range  $t_0 - T_0$ , as

$$\alpha = -0.932L^2m \quad (1)$$

where  $L$  is the half thickness of the disc. The curves

**Table 3.** Thermal properties of suspensions

| Property                                | Polystyrene            | Composition 1           | Composition 2          |
|---|------------------------|-------------------------|------------------------|
| Thermal diffusivity (m <sup>2</sup> /s) | 1.1 × 10 <sup>-7</sup> | 2.9 × 10 <sup>-7b</sup> | 4.0 × 10 <sup>-7</sup> |
| Specific heat <sup>a</sup> (J/kg K)     | 1700                   | 650                     | 920                    |
| Density (kg/m <sup>3</sup> )            | 1060                   | 3267                    | 2634                   |
| Softening point (°C)                    | 110                    | 58                      | 63                     |

<sup>a</sup>The specific heat was obtained as a function of temperature. The value quoted here corresponds to the glass transition temperature.

<sup>b</sup>From Ref. 22.

are plotted in Fig. 6. The resulting diffusivities are given in Table 3 along with the thermal diffusivity for composition 1 taken from previous work.<sup>22</sup> Specific heats at the glass transition temperature obtained from DSC measurements are also given in Table 3.

If the samples being welded are treated as symmetrical infinite flat plates with heat source  $\dot{q}$ , at the mid-plane, it is possible to calculate the time needed for the mid-plane to reach the softening point of the suspension. It is assumed that the initial temperature of the plate is 23°C and that heat is applied for such a short period (typically less than 2 s) that no heat is lost to the surroundings. A further assumption is that no heat is generated in the parent material, that is, ultrasonic attenuation in the bulk is neglected. The general equation of heat flow in each half plate is given by:

$$\rho C_p \frac{\partial T}{\partial t} = k \frac{\partial^2 T}{\partial x^2} + \dot{q} \quad (2)$$

where  $\dot{q}$  is the rate of heat generation per unit volume,  $\rho$  is the density of the suspension,  $C_p$  is specific heat,  $k$  is thermal conductivity, and  $x$  is distance perpendicular to the weld plane.

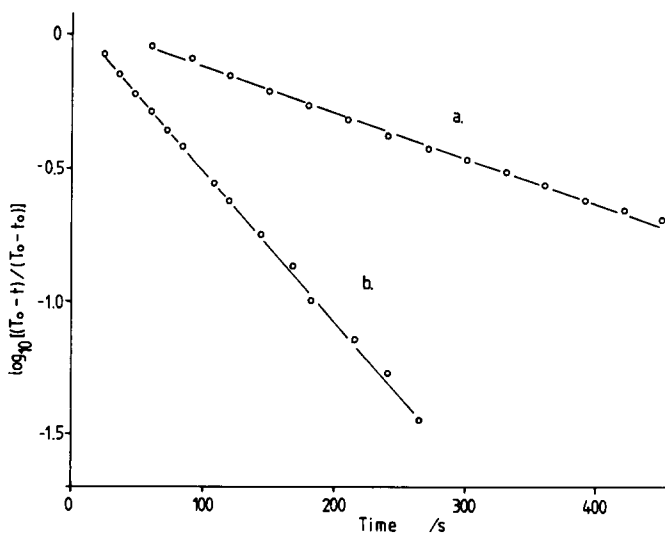


**Fig. 6.** Plots of logarithm of dimensionless temperature as a function of time for the measurement of thermal diffusivity for: (a) polystyrene ( $L = 8.50$  mm); (b) composition 2 ( $L = 8.75$  mm).

For the case where heat is generated at the interface by friction, the flux entering the first layer ( $n = 0$ ) of the mesh shown in Fig. 7 is  $\dot{q}/2$  where  $\dot{q}$  is now the total heat generated per unit area of the weld and is divided equally between the two adherends and  $\dot{q} = 0$  at all other points. Hence the general equation (eqn (2)) can be written in its finite difference form as:

$$T_{(x,t+\Delta t)} - T_{(x,t)} = r [T_{(x+\Delta x,t+\Delta t)} - 2T_{(x,t+\Delta t)} + T_{(x-\Delta x,t+\Delta t)}] \quad (3)$$

where

$$r = \alpha \Delta t / \Delta x^2 \quad \text{and} \quad \alpha = k / \rho C_p$$

which represents a general node. The boundary equation at the weldline is

$$T_{(0,t+\Delta t)} - T_{(0,t)} = \frac{1}{4} [T_{(1,t+\Delta t)} - T_{(0,t+\Delta t)}] + \dot{q} \Delta t / \rho C_p \Delta x \quad (4)$$

These equations were expressed as a set of tridiagonal matrices and solved for each time step  $\Delta t$ .<sup>23</sup> The advantage of using a finite difference solution rather than an analytical solution is that it allows the model to be developed further to accommodate heat dissipation in the bulk and thermal properties which vary with temperature.

A pure implicit method of solution was used because this is not prone to oscillating solutions and is unconditionally stable. Figure 8 shows the calculated temperature distributions in the joints for each material when the softening point was reached. The softening points were 58°C for composition 1<sup>22</sup> and 63°C for composition 2. A value of  $\dot{q}$  of  $6 \times 10^5$  W/m<sup>2</sup> was chosen for comparing different materials. This would mean that 10% of the overall

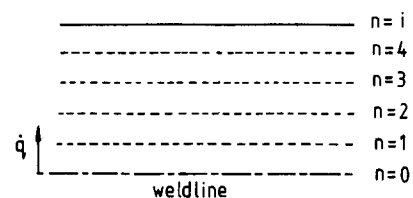


**Fig. 7.** Finite difference mesh for calculation of temperature distributions.

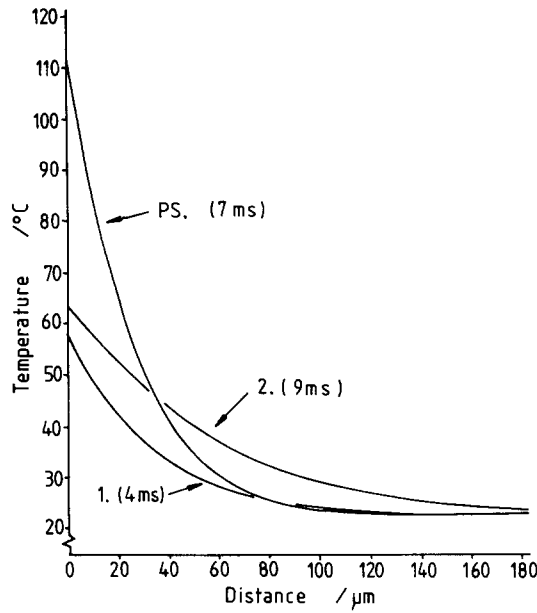


Fig. 8. Temperature distributions about the weldline at the time when the softening temperature is reached at the weldline.

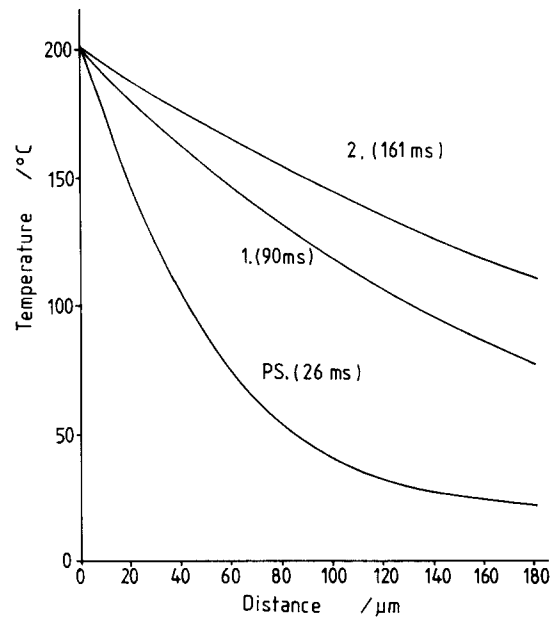


Fig. 9. Temperature distributions about the weldline at the time when the temperature at the weldline reached 200°C.

machine power was dissipated in the weld area. The calculation gives comparative results because the true value of this quantity was not obtained by calorimetry because of the considerable experimental difficulties.

Remembering that polystyrene is easily welded by this process, the temperature distributions of the filled polymers were compared with those for polystyrene. The presence of organic diluents in compositions 1 and 2 mean that  $T_g$  has been lowered. This has only a superficial advantage as discussed below, but Fig. 8 compares the temperature distributions at the point when  $T_g$  is reached at the weldline. This occurs at 4 ms for composition 1, 7 ms for polystyrene and 9 ms for composition 2. Although  $T_g$  represents the onset of flow it does not indicate that sufficient mobility exists to produce a weld.

For composition 1 at 45 vol.% loading, the relative viscosity for this powder would be 6.<sup>24</sup> A further comparison by calculation was therefore made at the time taken for the weldline to reach 200°C (corresponding to melt processing temperatures for polystyrene and the ceramic compositions). The distributions are shown in Fig. 9. This time the polystyrene takes 26 ms to reach 200°C compared to composition 1 which takes 90 ms. In both cases composition 2 is predicted to be the material most unreceptive to ultrasonic welding because of the higher loading of the alumina which confers a higher thermal diffusivity. It takes 161 ms for the interface to reach 200°C. Figure 9 emphasizes the deleterious effect of the enhanced thermal diffusivity of filled

polymers on ultrasonic welding. The heat sink provided by the bulk adherends abstracts heat from the interfacial region and means that longer weld times or greater power is needed. It also means that the bulk adherends are themselves melting with the consequence that considerable bulk deformation is to be expected before a weld can be produced.

It has been shown that an estimate of thermal conductivity,  $k^*$ , of a ceramic suspension can be obtained from the approximation that  $k_1 \gg k_2$  where subscripts 1 and 2 refer to the ceramic and polymer respectively using the relationship:<sup>25</sup>

$$k^* = k_2 \frac{1 + 2V_1}{1 - V_1} \quad (5)$$

Thus conductivity depends on the volume fraction  $V$  of the ceramic. Measured values of thermal conductivity obtained from thermal diffusivity compare well with estimated values using eqn (5) and are shown in Table 4. The implication is that ultrasonic welding of suspensions may only be suitable for compositions containing low ceramic volume fractions (<0.5).

The question, however, is whether heat abstraction from the weld zone is the main problem. In

Table 4. Estimated and measured thermal conductivities

|               | Thermal conductivity (W/mK) |           |
|---------------|-----------------------------|-----------|
|               | Measured                    | Estimated |
| Polystyrene   | 0.20                        | —         |
| Composition 1 | 0.62                        | 0.69      |
| Composition 2 | 0.97                        | 0.90      |

**Table 5.** Ultrasonic heating of bulk materials

|                             | Polystyrene   | Composition 1 | Composition 2 |
|-----------------------------|---------------|---------------|---------------|
| At 12.5 mm                  |               |               |               |
| $T(^{\circ}\text{C})$       | 2.4           | 8.9           | 11.4          |
| 95% CL <sup>a</sup> ( $n$ ) | $\pm 1.1(11)$ | $\pm 3.8(8)$  | $\pm 2.1(12)$ |
| $TC_p$ ( $\text{kJ/m}^3$ )  | 4350          | 19000         | 27600         |
| At 5 mm                     |               |               |               |
| $T(^{\circ}\text{C})$       | 4.4           | 4.4           | 16.3          |
| 95% CL ( $n$ )              | $\pm 1.8(7)$  | $\pm 4.5(3)$  | $\pm 3.1(5)$  |
| $TC_p$ ( $\text{kJ/m}^3$ )  | 8000          | 9300          | 39500         |

<sup>a</sup> Confidence limit.

order to shed some light on this question, the remaining impediments to welding must also be explored.

### 3.3 Ultrasonic attenuation in the bulk

Unfortunately, direct measurements of attenuation at 20 kHz could not be made and an alternative method was used. The heating of bulk compression moulded cylinders of compositions 1 and 2 and polystyrene were measured with central thermocouples after a fixed interval of continuous wave ultrasonic treatment in the welder. Table 5 shows the resulting temperature rises for central holes drilled 5 mm and 12.5 mm from the top surface. The ultrasound causes preferential heating locally at the thermocouple position and in order to avoid this erratic effect, the temperature rise was recorded after 1 min had elapsed allowing this local effect to disappear. The product of temperature rise and volume specific heat is also given so that the heat absorbed per unit volume can be compared for polystyrene and the two ceramic compositions. Typical temperature rise and cooling curves are shown in Fig. 10. Some measurements were made with the thermocouple (32 swg type K) inserted after

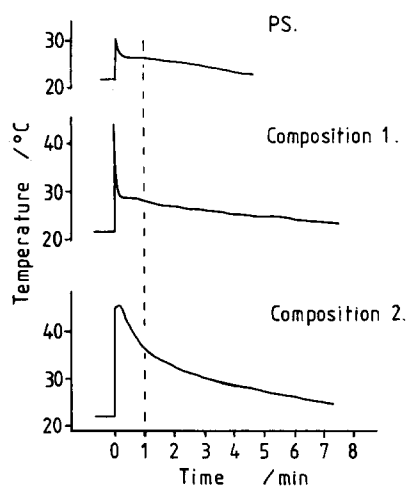


**Fig. 10.** Typical temperature fluctuations at the centre of the cylinders subjected to 2 s ultrasonic transmission.

ultrasound treatment had finished. They did not register a significantly different temperature after the 1 min lapse.

This experimental technique is not ideal and leads to wide scatter noted in the 95% confidence limits calculated from a student's  $t$  distribution for small populations. However, it gives a comparative measure of energy absorbed.

The results suggest that composition 1 experiences a slightly greater temperature rise than the polystyrene sample and that composition 2 experiences a much greater rise in temperature. The volumetric specific heat of composition 1 is only 18% higher than that for polystyrene and that for composition 2 is 34% higher. This accentuates the comparison but the temperature rise is the main indication of significant differences in attenuation.

The velocity of sound for longitudinal waves in bulk samples is given by:

$$C = \left[ \frac{E(1-\nu)}{\rho(1+\nu)(1-2\nu)} \right]^{1/2} \quad (6)$$

where  $E$  is elastic modulus and  $\nu$  is Poisson's ratio. Taking the effective elastic modulus  $E$  as 15 GPa at room temperature and  $\nu = 0.27$  for composition 1,<sup>26</sup>  $C = 2400$  m/s and the wavelength  $\lambda = 0.1$  m. When the particle size is small compared with the wavelength, Rayleigh scattering is possible. However, because the attenuation due to scattering is proportional to the fourth power of the frequency, Rayleigh scattering produces negligible attenuation at frequencies below 1 MHz<sup>27</sup> and viscous or thermal effects may predominate. This is in agreement with a study of ceramic-filled polyethylene at frequencies up to 40 MHz<sup>28</sup> wherein attenuation at low frequencies was indistinguishable for samples of different volume fraction.

In concentrated suspensions where an interaction between particles is possible, theories of attenuation are difficult to apply, but other studies show a strong dependence of attenuation on volume loading of dispersed phase in the MHz region.<sup>29</sup> Clearly, there is a need to relate attenuation to volume fraction and particle size experimentally for ceramic suspensions at welding frequencies. The greater weldability of composition 1 may be largely due to the lower ceramic volume loading since both suspensions contain mainly submicron particles. This is in conflict with the need to achieve high volume loadings for ceramics fabrication.

### 3.4 Coefficient of friction

It has been argued that a high coefficient of friction is desirable in materials to be ultrasonically welded.<sup>8</sup>



**Table 6.** Dynamic coefficients of friction

| Material  | Average $\mu$ |
|---|---------------|
| Polystyrene                                       | 1.4           |
| Composition 1                                     | 2.4           |
| Composition 2                                     | 2.7           |
| Polystyrene + Al <sub>2</sub> O <sub>3</sub> dust | 1.7           |

The effect of ceramic filler on coefficient of friction was therefore explored for polystyrene and the two ceramic compositions under reciprocating conditions with each material in contact with its own counterface. The measurement conditions are quite different to those encountered at the weld surfaces, nevertheless, gross differences between a filled and unfilled polymer should be revealed. The effect, for example, of equiaxed particles breaking away and acting as a solid lubricant should be manifested. Table 6 shows the dynamic coefficients of friction. In both cases the presence of ceramic filler increases the coefficient and the presence of ceramic powder sprinkled on polystyrene surfaces also increases the coefficient. It should, of course, be noted that compositions 1 and 2 also include plasticizers which may be responsible for modifying the behaviour. However, under the conditions used, the ceramic compositions offer an increased rather than a diminished coefficient.

#### 4 Conclusions

The ultrasonic welding of ceramic suspensions has been shown to be feasible by the observation of interfacial regions which are indistinguishable from the bulk. High quality sintered interfaces were obtained after binder removal and firing. However, there are difficulties with the welding operation which have yet to be overcome; notably the fracture of the samples under high amplitudes. The enhanced thermal diffusivity of ceramic suspensions has been shown to result in an undesirable low thermal gradient adjacent to the interface. Direct measurements of temperature rise show that the incorporation of ceramic powder increases the bulk heating caused by ultrasonic attenuation. These factors account for the narrower range of successful welding conditions which must be used for ceramic suspensions. In addition, it is speculated that increased melt viscosity caused by ceramic fillers may impede welding. Each of these adverse properties, embrittlement, thermal diffusivity, attenuation and viscosity, are closely related to the volume fraction of ceramic powder, suggesting, in conflict with fabrication requirements, that low ceramic volume fractions are desirable.

#### Acknowledgements

The authors are grateful to the late Professor R. E. D. Bishop for supporting this work under the Vice Chancellor's Earmarked Support for Research Scheme. Thanks are expressed to Mr K. Dutta for technical help with the friction measurements.

#### References

- Edirisinghe, M. J. & Evans, J. R. G., Systematic development of the ceramic injection moulding process. *Mater. Sci. Engng*, **A109** (1989) 17–26.
- Wright, J. K., Thomson, R. M. & Evans, J. R. G., On the fabrication of ceramic windings. *J. Mater. Sci.*, **25** (1990) 149–56.
- Haunton, K. M., Wright, J. K. & Evans, J. R. G., The vacuum forming of ceramics. *Br. Ceram. Trans. J.*, **89** (1990) 53–6.
- Hammond, P. & Evans, J. R. G., On the blow moulding of ceramics. *J. Mater. Sci. Lett.*, **10** (1991) 294–6.
- Rashid, H., Lindsey, K. A. & Evans, J. R. G., Joining ceramics before firing by solvent welding. *J. Eur. Ceram. Soc.*, **7** (1991) 259–65.
- Rashid, H. & Evans, J. R. G., Joining ceramics before firing by butt fusion welding. *Ceram. Int.* (in press).
- Wake, W. C., *Adhesives*. Royal Institute of Chemistry, London, Lecture Series No. 4, 1966, pp. 12–15.
- Wickham, M. J. & Watson, M. N., Welding Institute Members Report No. 336. The Welding Institute, Cambridge, UK, 1987.
- Blitz, J., *Elements of Acoustics*. Brunel University, UK, 1976, pp. 44–8.
- Tolunay, M. N., Dawson, P. R. & Wang, K. K., Heating and bonding mechanisms in ultrasonic welding of thermoplastics. *Polym. Engng Sci.*, **23** (1983) 726–33.
- Anon., Ultrasonic assembly of thermoplastic moulding and semi-finished products. ZVEI German Manufacturers Association, Frankfurt, undated.
- Potente, H., Ultrasonic welding; principle and theory. *Mater. Design*, **5** (1984) 228–34.
- Beatty, K. O., Armstrong, A. A. and Schoenburn, E. M., Thermal conductivity of homogeneous materials: Determination by an unsteady state method. *Ind. Engng Chem.*, **42** (1950) 1527–32.
- Hosseini, S. M. & Stolarski, T. A., Contact configuration effects on the dry and lubricated wear of polymers. *Surf. Engng*, **4** (1988) 322–6.
- Zhang, J. G., Edirisinghe, M. J. & Evans, J. R. G., The use of silane coupling agents in ceramic injection moulding. *J. Mater. Sci.*, **23** (1988) 2115–20.
- Zhang, T. & Evans, J. R. G., Mechanical properties of injection moulding suspensions as a function of ceramic volume fraction and temperature. *J. Eur. Ceram. Soc.*, **7** (1991) 155–63.
- Ishida, H., A review of recent progress in the studies of molecular and microstructure of coupling agents and their functions in composites, coatings and adhesive joints. *Polym. Compos.*, **5** (1984) 101–23.
- Manson, J. A., Interfacial effects in composites, *Pure Appl. Chem.*, **57** (1985) 1667–78.
- Zhang, T. & Evans, J. R. G., Predicting the viscosity of ceramic injection moulding suspensions. *J. Eur. Ceram. Soc.*, **5** (1989) 165–72.
- Gallagon, S. T., Laying the groundwork for ultrasonic welding. *Plast. Engng*, **41**(8) (1985) 35–7.

21. Wright, J. K., Edirisinghe, M. J., Zhang, J. G. & Evans, J. R. G., Particle packing in ceramic injection moulding. *J. Am. Ceram. Soc.*, **73** (1990) 2653–8.
22. Hunt, K. N., Evans, J. R. G. & Woodthorpe, J., Computer modelling of the origin of defects in ceramic injection moulding I. Measurement of thermal properties. *J. Mater. Sci.*, **26** (1991) 285–91.
23. Carnahan, B., Luther, H. R. & Wilkes, J. O., *Applied Numerical Methods*. John Wiley, New York, 1969, pp. 441–2, 452–61.
24. Hunt, K. N., Evans, J. R. G. & Woodthorpe, J., The influence of mixing route on the properties of ceramic injection moulding blends. *Br. Ceram. Trans. J.*, **87** (1988) 17–21.
25. Zhang, T., Evans, J. R. G. & Dutta, K. K., Thermal properties of ceramic injection moulding suspensions in the liquid and solid states. *J. Eur. Ceram. Soc.*, **5** (1989) 303–9.
26. Hunt, K. N., Evans, J. R. G., Mills, N. J. & Woodthorpe, J., Computer modelling of the origin of defects in ceramic injection moulding IV. Residual stresses. *J. Mater. Sci.*, **26** (1991) S229–S238.
27. Blitz, J., *Fundamentals of Ultrasonics*. Butterworths, London, 1963, pp. 150–3.
28. Bridge, B., Ultrasonic non-destructive evaluation of hydroxyapatite-filled polyethylene, a novel prosthetic material. *Br. J. NDT*, **29** (1987) 417–25.
29. Richardson, E. G., *Ultrasonic Physics*, 2nd edn. Elsevier, Amsterdam, 1962, pp. 263–8.